Synthetic Lethal Screening Identifies Compounds Activating Iron-Dependent, Nonapoptotic Cell Death in Oncogenic-RAS-Harboring Cancer Cells

Wan Seok Yang[1] and Brent R. Stockwell[1,2,*]
[1]Department of Biological Sciences
[2]Department of Chemistry
Columbia University, Fairchild Center, MC2406, 1212 Amsterdam Avenue, New York, NY 10027, USA
*Correspondence: stockwell@biology.columbia.edu
DOI 10.1016/j.chembiol.2008.02.010

SUMMARY

We screened small molecules to identify two compounds, which we named RSL3 and RSL5, that have increased lethality in the presence of oncogenic RAS. Counter screening with biologically active compounds defined aspects of the mechanism of action for RSL3 and RSL5, such as a nonapoptotic, MEK-dependent, and iron-dependent oxidative cell death. Erastin, a previously reported compound with RAS-selective lethality, showed similar properties. RNA interference experiments targeting voltage-dependent anion channel 3 (*VDAC3*), a target of erastin, demonstrated that RSL5 is a scaffold that acts through VDACs to activate the observed pathway. RSL3 activated a similar death mechanism but in a VDAC-independent manner. We found that cells transformed with oncogenic RAS have increased iron content relative to their normal cell counterparts through upregulation of transferrin receptor 1 and downregulation of ferritin heavy chain 1 and ferritin light chain.

INTRODUCTION

Leads for new cancer therapeutics often emerge from target-based, in vitro screening. Targeted kinase inhibitors, such as Gleevec and Iressa have been effective in treating tumors by using a targeted therapy approach. However, many proteins cannot be targeted with enzymatic, active-site inhibitors. RAS, the most frequently mutated oncogene, is mutated in a way that causes loss of its GTPase activity, thereby activating downstream effectors of RAS pathways. Restoring GTPase function to mutant RAS with pharmacological agents is a challenging task compared to the traditional approach of discovering enzyme inhibitors.

To circumvent this problem, efforts have been made to target related signaling pathways instead of the mutant protein per se. For example, oncogenic RAS cannot hydrolyze bound GTP and consequently binds downstream signaling proteins, including RAF, PI3K, RalGDS, and PLCε in its GTP-bound form. As activation of multiple downstream signaling molecules are crucial to RAS-mediated tumorigenesis and tumor maintenance, discovery of inhibitors targeting these downstream molecules may lead to novel anticancer drugs: Sorafenib (Wilhelm et al., 2006),

a RAF kinase inhibitor, was approved by the FDA in the U.S. for the treatment of renal cell carcinoma.

Nonetheless, to date, efforts to target RAS signaling have been focused mostly on target-based, in vitro screening. RAS is proposed to interact with more than 360 proteins (Bernards, 2005), and it is possible that distal downstream components of the oncogenic-RAS-signaling network could be targets for drug discovery. A strategy for revealing these critical RAS-linked targets is synthetic lethal screening (Hartwell et al., 1997). For a given mutation "A," if there exists a second mutation "B" that is particularly lethal to the organism in the presence of A, mutation B is synthetic lethal with mutation A because the lethality requires the synthesis, or bringing together, of the two mutations. In synthetic lethal screening with oncogenic RAS, the second perturbation can be created by using a small molecule to alter the function of a target protein rather than by introducing a mutation in the gene encoding the protein (Figure 1A; Stockwell, 2000).

The existence of striking synthetic lethal interactions in genome-wide studies has been demonstrated with yeast deletion strains (Tong et al., 2001). Each yeast gene has on average 30 synthetic lethal/sick interactions with other yeast genes. In anticancer therapeutics, several compounds have been reported to display synthetic lethality, including (1) RB with topoisomerase II inhibitors (Banerjee et al., 1998), (2) PTEN with mTOR inhibitors (Neshat et al., 2001), and (3) BRCA1 with PARP inhibitors (Bryant et al., 2005). In accord with the concept of synthetic lethality, cancer cells with mutations in RB, PTEN, or BRCA1 are more sensitive to the respective compound treatments than normal cells without such mutations.

We have pursued synthetic lethal screening with small molecules to identify those that display synthetic lethality with oncogenic RAS; we reported that the compound erastin has this property (Dolma et al., 2003). As expected, the target of erastin is not RAS itself: erastin binds to voltage-dependent anion channels, a novel target for anticancer drugs, to induce RAS-RAF-MEK-dependent oxidative, nonapoptotic cell death (Yagoda et al., 2007).

We used a series of engineered cell lines derived from primary human fibroblasts for screening (Figure 1B; Dolma et al., 2003; Hahn et al., 1999). Briefly, BJ cells were engineered successively to express the catalytic subunit of human telomerase (hTERT), the SV40 large T and small T antigens (LT and ST), and an oncogenic allele of HRAS (HRAS^G12V). We named these cells lines BJ-TERT, BJ-TERT/LT/ST, and BJ-TERT/LT/ST/RAS^V12. Only the BJ-TERT/LT/ST/RAS^V12 cells form tumors in nude mice.
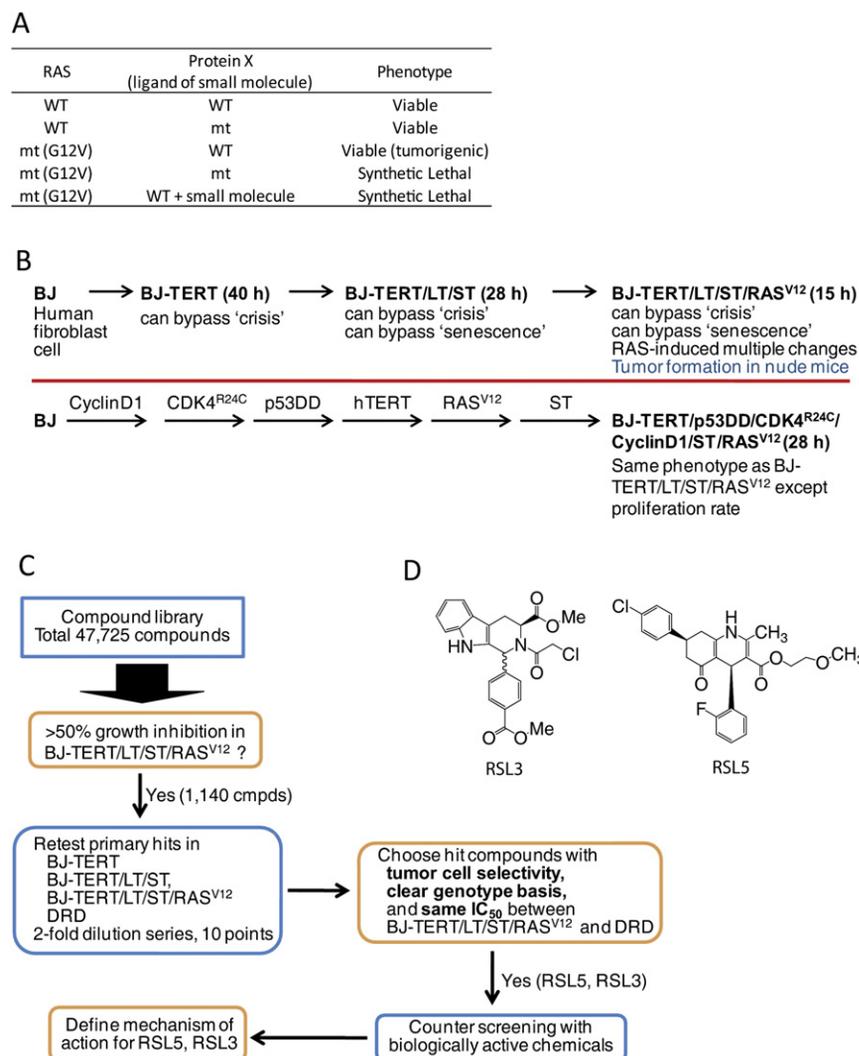
Figure 1. Overview of Our Synthetic Lethal Screening Strategy

(A) Two genes (in this case, RAS and Protein X, a target of a small molecule) are synthetic lethal if perturbations in either alone has little consequence to the cell, but simultaneous perturbation of both causes death. Perturbation of protein X can be produced by either genetic mutation or small-molecule treatment.

(B) Characteristics of isogenic cell lines used for synthetic lethal screening. Sequential introduction of oncogenic elements converts human primary fibroblast cells into tumorigenic cells. Phenotypic changes associated with expression of each genetic element are indicated along with cell doubling time. Both RAS^{V12} harboring cells (BJ-TERT/LT/ST/RAS^{V12} and BJ-TERT/p53DD/CDK4/cyclinD1/ST/RAS^{V12} cells) can form tumors in nude mice but differ in cell doubling time, which allows filtering out proliferation-rate-dependent lethal compounds.

(C) Flow chart of our screening strategy.

(D) Structure of RSL5 and RSL3.

that are either synthetic or natural-product derivatives. All compounds were tested in BJ-TERT/LT/ST/RAS^{V12} cells in 384-well plates (one compound per well) at a concentration of 5 μg/ml, corresponding to 13 μM for a compound with a molecular weight of 400. After 2 days of incubation, cell viability was assessed with alamar blue, which detects changes in cellular reductive potential (Nociari et al., 1998).

Compounds that inhibited alamar blue metabolism in BJ-TERT/LT/ST/RAS^{V12} cells more than 50% were considered initial hits and tested in an extensive 2-fold dilution series in BJ-TERT/LT/ST/RAS^{V12} cells and in isogenic cells lacking oncogenic RAS (BJ-TERT and BJ-TERT/LT/ST) and in a nearly isogenic, tumorigenic cell line that grows slowly (BJ-TERT/p53DD/CDK4/cyclinD1/ST/RAS^{V12} cells, hereafter, DRD cells, see below).

We refined this screening system by incorporating DRD cells, which were engineered to express hTERT, SV40 small T oncoprotein, oncogenic HRAS (HRAS^{G12V}), dominant negative p53, and constitutively active CDK4/cyclinD, which inactivates the RB protein. The p53DD/CDK4/cyclinD1 combinations substitute for the SV40 large T oncoprotein (Figure 1B; Dolma et al., 2003; Hahn et al., 2002). Given that DRD cells are also derived from BJ primary cells and the effects of mutations in both lines should be similar, ideal synthetic lethal compounds should have similar growth inhibitory potency in DRD cells and BJ-TERT/LT/ST/RAS^{V12} cells. Both BJ-TERT/LT/ST/RAS^{V12} cells and DRD cells form tumors in nude mice, but the doubling time of DRD cells is significantly longer than that of BJ-TERT/LT/ST/RAS^{V12} cells in vitro (Figure 1B). Thus, the use of DRD cells as a counter screen enabled us to eliminate compounds that (1) have idiosyncratic activity in BJ-TERT/LT/ST/RAS^{V12} cells, (2) are simply

Our screening was aimed at identifying compounds lethal to BJ-TERT/LT/ST/RAS^{V12} cells while having minimal effects on their isogenic cell precursors. It should be noted that while we used oncogenic HRAS in the primary screen, we tested all hit compounds for their selectivity against oncogenic KRAS, which is more commonly mutated in human cancers.

Here, we report the results of screening using a refined cell line system, a novel collection of small molecules, and a systematic analysis of mechanism of action. We identified two novel small molecules that have synthetic lethal interactions with mutant RAS and characterized their mechanism of action, which lead to the discovery that oncogenic RAS signaling enriches the cellular iron pool by modulating the iron metabolism network.

RESULTS

Identification of Small Molecules that Are Synthetic Lethal to Oncogenic RAS

We developed a new screening cascade for discovering genetically selective compounds and ruling out proliferation-dependent compounds (Figure 1C). We collected 47,725 compounds

Figure 2. Effect of RSL5 on Four BJ-Derived Cell Lines and Results of Counter Screening with Bioactive Molecules

(A) BJ-TERT, BJ-TERT/LT/ST, BJ-TERT/LT/ST/RAS^{V12}, and DRD cells were treated with RSL5 in 384-well plates for 48 hr. Error bars indicate one standard deviation of triplicate data.

(B and C) BJ-TERT/LT/ST/RAS^{V12} cells were treated with RSL5 in the presence of the indicated bioactive molecules in 384-well plates for 24 hr. The concentration of each bioactive compound is listed in Table S1. Percent growth inhibition was measured with alamar blue. The graph is a representative outcome of multiple experiments.

Figure 3. Effect of RSL3 on Four BJ-Derived Cell Lines and Results of Counter Screening with Bioactive Molecules

(A) BJ-TERT, BJ-TERT/LT/ST, BJ-TERT/LT/ST/RAS^{V12}, and DRD cells were treated with RSL3 in 384-well plates for 48 hr. Data represents the mean ± SD of triplicate samples.

(B and C) BJ-TERT/LT/ST/RAS^{V12} cells were treated with RSL3 in the presence of indicated bioactive compounds in 384-well plates for 24 hr. The concentration of each bioactive compound was listed in Table S1. Percent growth inhibition was measured with alamar blue. The graph is a representative outcome of multiple experiments.

more potent in rapidly dividing cells, or (3) are dependent on the SV40 viral protein rather than an endogenous oncogenic signaling pathway.

After analyzing the results of the 2-fold dilution series testing, we picked two novel compounds, which we have named RSL3 and RSL5, for oncogenic-*RAS*-*s*elective *l*ethal compounds, as our final hits, because they displayed synthetic lethality with oncogenic RAS in both BJ-TERT/LT/ST/RAS^{V12} and DRD cells (Figure 1D). We confirmed the cell killing effect of these compounds by using a trypan blue assay (see below). The presence of oncogenic RAS signaling is required for more efficient cell killing by these compounds. The IC$_{50}$ value in BJ-TERT/LT/ST/RAS^{V12} cells was similar to that in DRD cells, which indicates that the syn-

thetic lethal interaction is relevant beyond a single cell line (Figures 2A and 3A) and that the compounds are not proliferation dependent in their activity. Thus, this screening cascade yielded two novel compounds that have a degree of synthetic lethality with oncogenic RAS.

Mechanism of Action Study with a Set of Biologically Active Molecules

To assess potential mechanisms of action underlying cell death induced by RSL5 and RSL3, our strategy was to test a series of biologically active compounds for their ability to suppress cell death induced by RSL3 or RSL5. This is akin to a genetic suppressor screen, except that we are making use of small molecules in place of mutations. The compounds were chosen based on their reported ability to inhibit aspects of cell death signaling

(z-VAD-fmk, Boc-D-fmk, vitamin E, reduced gluthathione [GSH], desferrioxamine mesylate [DFOM], and cycloheximide [CycH]) or kinase signaling related to RAS (U0126, SB203580, Wortmannin, Rapamycin, and SU6656) (see Table S1 in the Supplemental Data available with this article online for detailed information).

We treated BJ-TERT/LT/ST/RAS^{V12} cells with an individual bioactive compound, along with either RSL5 or RSL3, and monitored changes in cell sensitivity (Figures 2B, 2C, 3B, and 3C). RSL5 and RSL3 shared many properties. First, caspase inhibitors (z-VAD-fmk, Boc-D-fmk) were not effective at suppressing cell death induced by RSL3 or RSL5, despite the fact that these pan-caspase inhibitors efficiently suppress cell death induced by other apoptotic stimuli (Varma et al., 2007); therefore, RSL5-induced and RSL3-induced cell death is caspase independent (Figures 2B and 3B).

Second, an iron chelator (DFOM) and an antioxidant (vitamin E) were able to inhibit RSL5-induced and RSL3-induced cell death, suggesting involvement of Fenton chemistry and reactive oxygen species (ROS) (Figures 2B and 3B).

Third, a SRC kinase inhibitor (SU6656) blocked RSL5-induced cell death and suppressed RSL3-induced cell death (Figures 2C and 3C). SRC kinase is known to act as an upstream regulator of the RAS signaling pathway (Smith et al., 1986). Thus, treatment with this SRC kinase inhibitor likely attenuates oncogenic RAS signaling.

Finally, a MEK1/2 inhibitor (U0126) was able to suppress RSL5-induced and RSL3-induced cell death, demonstrating that it is specifically the RAS-RAF-MEK pathway that causes RSL5 and RSL3 sensitivity, as opposed to other aspects of RAS signaling. For example, a PI3K inhibitor (wortmannin), an mTOR inhibitor (rapamycin), and a SAPK inhibitor (SB203580) were all without effect on sensitivity to RSL5 and RSL3 (Figures 2C and 3C).

While RSL5 and RSL3 share a number of properties, we did see some differences upon protein-synthesis inhibitor (CycH) treatment (Figures 2B and 3B). RSL5 required protein synthesis to induce cell death, while RSL3 did not.

Both BJ-TERT/LT/ST/RAS^{V12} cells and DRD cells are engineered cell lines. To test the effect of these compounds in genuine tumor cells, we explored their lethality in HT1080 cells. Our goal was to determine whether the oncogenic-RAS-signal dependent lethality of RSL5 and RSL3 was relevant beyond these engineered cell lines. HT1080 cells originate from a human fibrosarcoma, contain an oncogenic RAS mutation (NRAS Q61A), and are tumorigenic in nude mice. In these experiments, we included erastin, which we previously reported as an inducer of synthetic lethality with oncogenic RAS. We found previously that erastin induces RAS-RAF-MEK-dependent oxidative cell death (Yagoda et al., 2007).

Bioactive compounds that suppressed RSL5 or RSL3 (DFOM, vitamin E, CycH, U1026, and SU6656) were tested against erastin, RSL5, and RSL3 in HT1080 cells (Figure S1). All three lethal compounds were suppressed by the SRC inhibitor (SU6656) and the MEK inhibitor (U0126), confirming the RAS-RAF-MEK-dependent lethality in these HT1080 cells. Antioxidants (e.g., vitamin E) and iron chelators (e.g., DFOM) were able to suppress cell death induced by these three lethal compounds. Therefore, all three compounds (erastin, RSL5, and RSL3) induce a similar phenotype, that is, a RAS-RAF-MEK-dependent oxidative, iron-dependent cell death. However, a protein synthesis inhibitor (CycH) was able to suppress cell death induced by erastin and RSL5, but not RSL3, implying the precise mechanism of action of RSL5 and RSL3 might be different (Figure S1).

Involvement of VDAC3 in Erastin-Induced and RSL5-Induced Cell Death

As erastin, RSL5, and RSL3 emerged from a similar screening setting and share a common genetic selectivity and induced phenotype, we wanted to determine whether RSL5 and RSL3 act through the same mechanism as erastin, by engaging mitochondrial VDACs. By using affinity purification and mass spectrometry, mitochondrial voltage-dependent anion channels (VDACs) were identified as specific targets of erastin (Yagoda et al., 2007).

Mammalian cells have three VDAC isoforms, VDAC1, VDAC2, and VDAC3. An erastin affinity analog specifically purified VDAC2 and VDAC3 only in lysates of BJ-TERT/LT/ST/RAS^{V12} cells, not of BJ-TERT cells. RNA interference experiments targeting VDAC2 and VDAC3 demonstrated that erastin binding to VDAC2 and VDAC3 induces a gain-of-function lethality: knocking down VDAC3 makes cells resistant to erastin, and knocking down VDAC2 reduces their sensitivity to erastin (Yagoda et al., 2007).

To test the possibility of VDAC involvement in the synthetic lethal action of RSL5 and RSL3, we knocked down VDAC3 in HT1080 cells by using short hairpin RNAs (shRNAs) specifically targeting *vdac3*. Knockdown of VDAC3 protein suppressed erastin-induced and RSL5-induced cell death, whereas RSL3 lethality was not affected (Figure 4). Introduction of shRNAs targeting *VDAC3* did not change the level of other VDAC isoforms (VDAC1 and VDAC2), as assessed by quantitative PCR (Q-PCR) (Figure S2). Thus, RSL5 acts through at least VDAC3, as does erastin. However, RSL3 appears to act in a VDAC-independent manner. This is significant, because it demonstrates that the oxidative, nonapoptotic cell death pathway targeted by these compounds is not restricted to VDAC involvement but can be activated under other conditions and may be more generally important.

RSL3 Has Oncogenic-RAS-Signal Dependent Lethality with a Unique Sensitivity Profile

RSL3's ability to induce synthetic lethality with oncogenic RAS was rapid and quite potent. This compound inhibited the growth of BJ-TERT/LT/ST/RAS^{V12} and DRD cells as low as 10 ng/ml (Figure 3A) and started to kill sensitive cells as early as 8 hr after treatment (Figures 5A and 5C). We carried out a trypan blue exclusion assay to confirm the growth inhibitory effect and the selectivity of RSL3. This was performed in a Vi-Cell (Beckman Coulter), which stains cells with trypan blue, takes 100 images, and analyzes the images to calculate the number of viable cells (i.e., cells excluding trypan blue). This assay eliminates false positives caused by autofluorescence or redox activity from a compound in the alamar blue assay. The trypan blue exclusion assays with RSL3 revealed a similar level of potency and selectivity as the alamar blue assay (Figure 5B). Moreover, longer treatment with RSL3 had little effect on the viability of cells lacking oncogenic RAS, confirming the qualitative nature of RSL3's selectivity (Figure 5B).
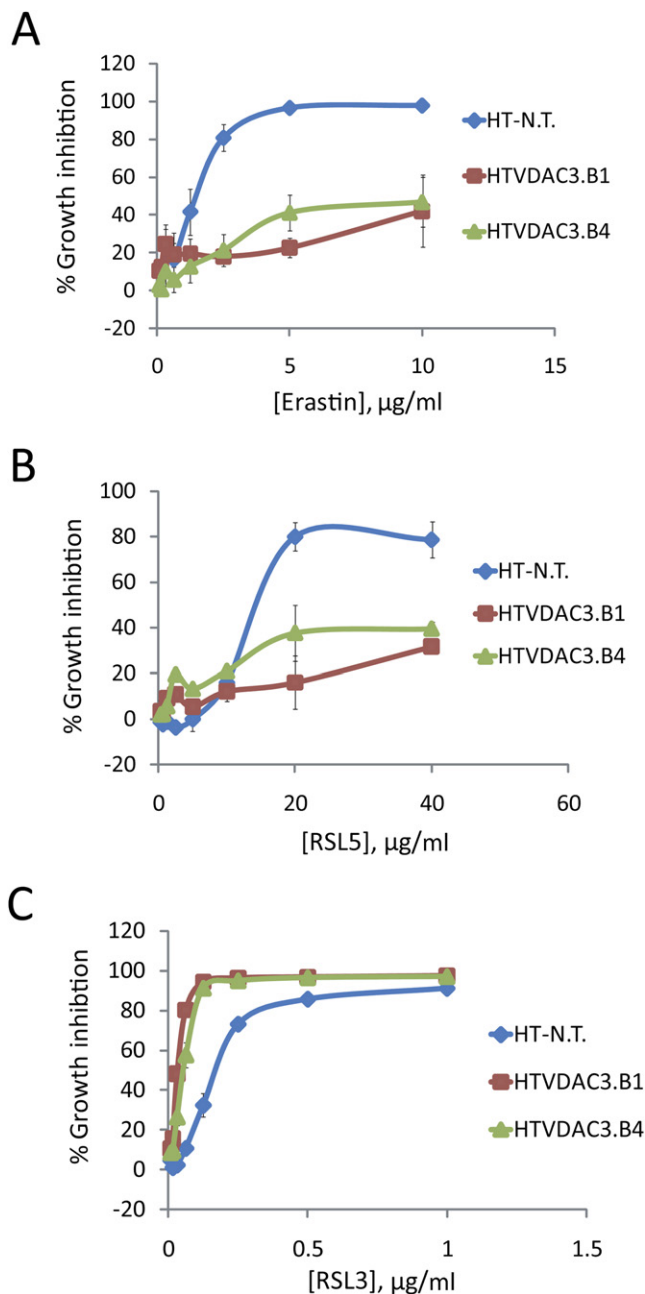
Figure 4. RSL5 and Erastin Utilize VDAC3 to Create Synthetic Lethality with RAS

HT1080 cells were infected with lentivirus-encoding shRNAs targeting *VDAC3* and treated with erastin (A), RSL5 (B), or RSL3 (C). Expression of shRNAs targeting *VDAC3* prevented cell death caused by RSL5 and erastin, whereas the sensitivity of RSL3 was not changed. Percent growth inhibition was determined with alamar blue. Error bars indicate one standard deviation of triplicate data.

Cell death induced by RSL3 treatment was not blocked by pan-caspase inhibitors (z-VAD-fmk, Boc-D-fmk), suggesting that a caspase-independent death pathway is involved in RSL3-induced cell death (Figures 2B and 3B). Because the survival effect of caspase inhibitors can be masked by activation

of alternative cell death pathways upon drug treatment, we employed a more sensitive measurement of caspase activation to examine the possible involvement of caspases in RSL3-induced cell death. Poly(ADP-ribose) polymerase-1 (PARP-1) is an abundant nuclear enzyme that is subject to cleavage by activated caspase 3/7. We compared staurosporine, erastin, RSL5, and RSL3 treatments of BJ-TERT/LT/ST/RAS[V12] cells, prepared cell lysates, and analyzed PARP-1 cleavage by western blot with an anti-PARP-1 antibody (Figure 5D). Only staurosporine-treated sample showed PARP-1 cleavage, indicating that staurosporine induces classical apoptotic cell death involving caspases, whereas erastin, RSL5, and RSL3 activate a nonapoptotic pathway (Figure 5D).

Among the three *RAS* genes (*HRAS*, *KRAS*, *NRAS*), the BJ cell system employed *HRAS* mutations to initiate oncogenic signals. All three RAS proteins can activate common downstream effectors but, for elusive reasons, human cancer cells have biased mutation rates among the three *RAS* genes; more than 70% contain *KRAS* mutations, 25% *NRAS* mutations, and less than 5% *HRAS* mutations (Rodenhuis, 1992). Since *KRAS* mutations are the most prevalent in human cancers, we tested the activity of RSL3 in *KRAS*-mutation-harboring cancer cells (Figure 6A). This compound was active in all oncogenic-KRAS-harboring cancer cell lines tested (Figure 6A). Among them, Calu-1 cells were the most sensitive to RSL3 (Figure 6A); the IC$_{50}$ in Calu-1 cells was 20 ng/ml.

Considering RSL3's high potency, we reasoned it would be interesting to test this compound in a broader range of cancer cell lines and see if there exist additional cell lines, like Calu-1, that are particularly sensitive. We submitted RSL3 to the Developmental Therapeutics Program (DTP) at the NCI in order to test this possibility. RSL3 was tested in 60 different human cancer cell lines (the NCI60 panel), and the growth inhibitory potency of RSL3 was determined across these cell lines. A number of cell lines were particularly sensitive to RSL3 treatment; nanomolar concentrations of RSL3 were often sufficient to induce growth arrest or cell killing, and there was up to 10^4-fold differences in sensitivity between resistant and sensitive cell lines (Figure 6B and Figure S3). Moreover, the sensitivity profile of RSL3 across the 60 cancer cell lines was distinct from those of known compounds in the NCI database, as assessed by the COMPARE algorithm (Paull et al., 1989), which suggests the mechanism of action for RSL3 is unique (Figure 6B). The COMPARE algorithm compares sensitivity profiles of an input compound to those of all other compounds in the database and returns a similarity score in terms of pairwise correlation coefficient (PCC). In control tests, the sensitivity profile of paclitaxel grouped with vinblastine, maytansine, and rhizoxin, with high PCC values (Figure 6B). All of these compounds are known to perturb microtubule integrity, which demonstrates the usefulness of the COMPARE algorithm to understand the mechanism of compound action. In contrast, the COMPARE analysis of RSL3 returned only compounds with low PCC values (Figure 6B). In other words, no compounds in the NCI database had a similar pattern of cell killing as RSL3.

We inferred that the oncogenic-RAS-signal-dependent lethality of RSL3 should persist in cancer cell lines other than *HRAS*-transformed fibroblasts, because the protein target of RSL3 is not HRAS itself, but is a protein associated with the oncogenic

RAS network whose status changes upon activation of oncogenic RAS signaling, regardless of subtype of RAS (H, N, or KRAS) or tissue origin (sarcomas or carcinomas). To test this hypothesis, we cultured Calu-1 cells, which were derived from a human lung carcinoma, and attenuated oncogenic RAS signaling by using shRNAs targeting *HRAS*, *NRAS*, or *KRAS*. RSL3 became less effective in Calu-1 cells expressing shRNAs targeting each RAS isoform, regardless of subtype (Figure 6C). Treatment with shRNAs targeting RAS isoforms did not lead to a general survival effect, since we did not observe loss of sensitivity to staurosporine (Figure S4).

Oncogenic RAS Signaling Enriches the Cellular Iron Pool by Regulating Expression Levels of *TfR1*, *FTH1*, and *FTL*

It was of interest that all RSLs were inhibited by an iron chelator, DFOM. We decided to test an additional iron chelator, compound 311 (Green et al., 2001), to test whether the protective effect of DFOM comes from its ability to deplete iron, or from other factors that may be specific to DFOM. We were able to confirm depletion of the cellular iron pool by both iron chelators with the fluorescent iron sensor, Phen Green SK (PGSK) (data not shown). This cell-permeable dye has green autofluorescence, which diminishes upon binding to cellular iron (Petrat et al., 2000). Thus, we saw increased fluorescence intensity in iron-chelator-treated BJ-TERT/LT/ST/RAS^{V12} cells. When we treated these cells with RSLs in the presence of these iron chelators, the activities of the RSLs were significantly inhibited, highlighting the importance of iron levels for inducing lethality (Figure 7A).

We reasoned that these engineered tumor cells might have increased iron content compared to their nontumorigenic counterparts, causing us to identify iron-dependent lethal compounds in this screen for synthetic lethality. To test this hypothesis, we examined cellular iron levels by using PGSK (Figure 7B). When we detected the intensity of fluorescence from PGSK-treated BJ cells by flow cytometry, we found that BJ-TERT and BJ-TERT/LT/ST cells showed a similar profile, whereas BJ-TERT/LT/ST/RAS^{V12} cells showed decreased fluorescence (Figure 7B). This indicates that BJ-TERT/LT/ST/RAS^{V12} cells have a greater basal level of iron than their isogenic precursors.

We suspected that iron-metabolism-related proteins in BJ-TERT/LT/ST/RAS^{V12} cells might be altered to allow increased iron uptake and maintenance in response to introduction of oncogenic RAS. Transferrin receptor 1 (TfR1) is a membrane protein that binds to the transferrin-iron complex and is internalized to release iron within the cytoplasm (Cheng et al., 2004). We monitored the expression level of *TfR1* by western blot and detected an increase in BJ-TERT/LT/ST/RAS^{V12} (Figure 7C). Thus, one explanation as to how BJ-TERT/LT/ST/RAS^{V12} cells exhibit greater levels of iron is that they have more TfR1, which leads to increased iron uptake.

We wanted to validate the importance of iron in RSL-induced cell death by reducing iron levels by a genetic method and then comparing drug sensitivity between the modified cell line and the parental cell line. Three different shRNAs targeting *TfR1* were delivered to BJ-TERT/LT/ST/RAS^{V12} cells by a lentiviral system (Moffat et al., 2006). Two shRNA clones displayed moderate level of knock down efficiency (clone 658 and 659), whereas one shRNA clone was not effective, as assessed by western

blot analysis (clone 660) (Figure 7D). When we tested erastin in these cells, erastin became less effective in clone-658-expressing and clone-659-expressing cells, compared to clone-660-expressing and nontargeting-shRNA-expressing cells (Figure 7E). However, the level of cell death suppression was not comparable to that of iron-chelator-treated cells (compare Figures 7A and 7E). This partial rescuing activity of shRNAs targeting TfR1 may reflect insufficient level of knock down or the existence of other mechanisms for enriching the iron content of RAS-transformed cells.

To explore other aspects of oncogenic-RAS signaling relevant to iron enrichment, we compared the expression level of other genes whose functions are known to modulate cellular iron content. The TfR1-mediated pathway is one route of iron uptake, but the cellular iron pool is also controlled by an iron storage protein complex, consisting of ferritin heavy chain 1 (FTH1) and ferritin light chain (FTL) (Harrison and Arosio, 1996). Real-time RT-PCR analysis showed a gradual increase in *TfR1* mRNA levels across the BJ-TERT, BJ-TERT/LT/ST, and BJ-TERT/LT/ST/RAS^{V12} cells, in agreement with western blot analysis (Figures 7F and 7C). Interestingly, the expression level of both *FTH1* and *FTL* was specifically decreased in BJ-TERT/LT/ST/RAS^{V12} cells (Figure 7F), indicating that oncogenic-RAS-signaling has a dual-prong mechanism to augment the cellular labile iron pool: one is to increase iron uptake via upregulation of *TfR1*, the other is to reduce the capacity of iron storage via downregulation of *FTH1* and *FTL*.

DISCUSSION

In this synthetic lethal screening system, we used oncogenic RAS (HRAS^{G12V}, although all hits were tested for oncogenic-KRAS-selectivity); we searched for compounds with increased lethality in the presence of this mutation. It is possible that some hits from such a screen might have selectivity toward HRAS, but not other RAS isoforms; such small molecules are potentially useful research tools to define differences in downstream signaling pathways activated by different RAS isoforms. Even in this case, it is important to note that the target protein for the compound would be very unlikely to be HRAS^{G12V} itself. According to the concept of synthetic lethality, one mutation is HRAS^{G12V}, and the hit compound simulates a second mutation in gene *B* by binding to protein B (Figure 1A).

This implies that a synthetic lethal screening strategy enables us to target the oncogenic-RAS-signaling pathway, without inhibiting RAS proteins themselves, which provides a broader range of targets in a single screen compared to conventional target-based in vitro screening. For example, these novel compounds (RSL5 and RSL3) display RAS-RAF-MEK-signal-dependent activity. As all three RAS isoforms can activate downstream RAF-MEK signaling cascades, the synthetic lethality of RSL5 and RSL3 is not limited to HRAS^{G12V}. We demonstrated this isoform-independent action of RSL3 by using shRNAs targeting the three RAS genes in a lung-carcinoma-derived cell line (Figure 6C). It should be noted that due to the remoteness of the target protein from RAS, other oncogenes may also sensitize cells to these RSL compounds if they activate signaling pathways largely overlapping with RAS.
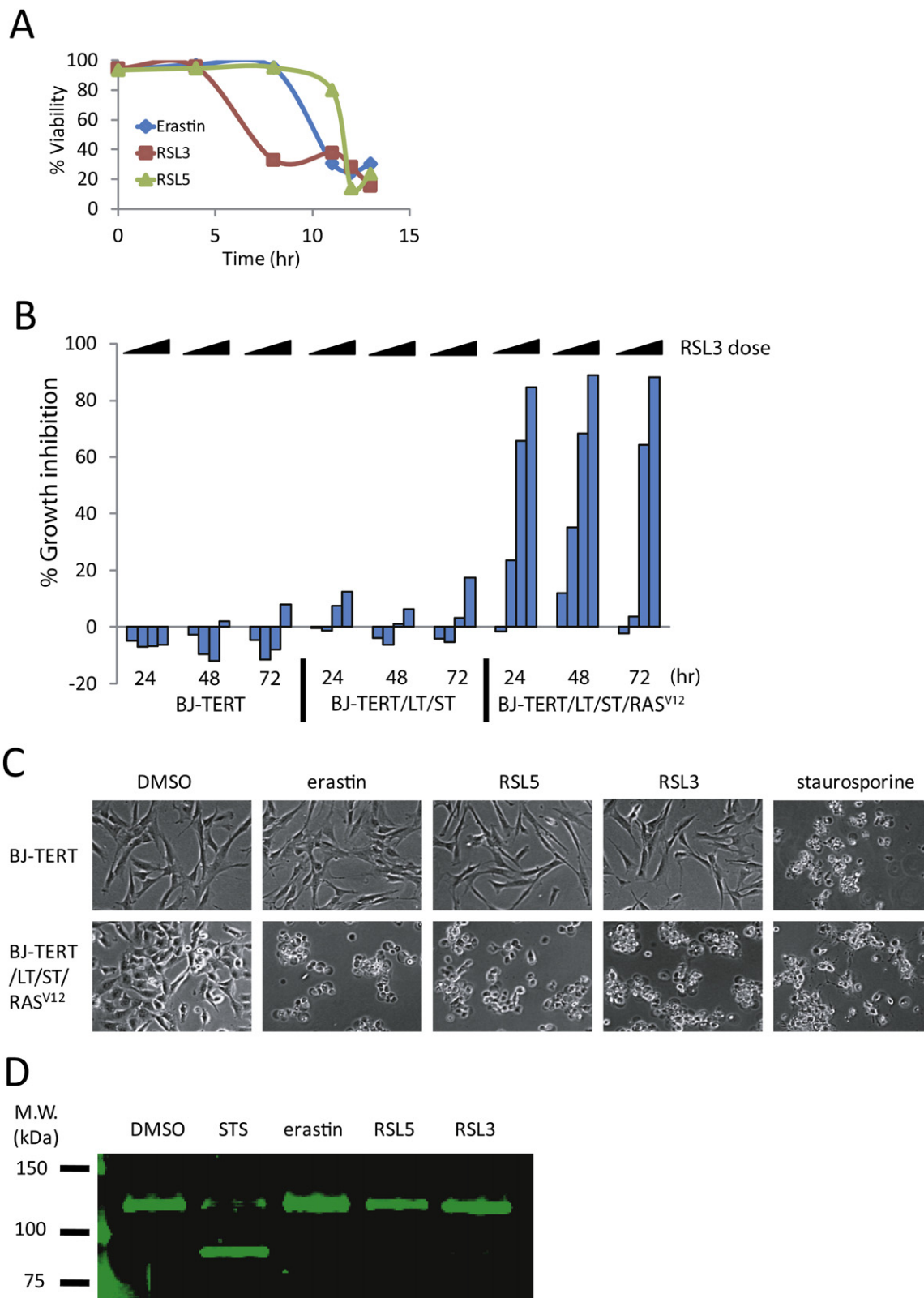
Figure 5. RSL3 Induces Rapid and Nonapoptotic Cell Death in Oncogenic RAS Containing Tumorigenic Cells

(A) Kinetic analysis of cell death induced by erastin, RSL5, and RSL3. RSL3 induced growth inhibition as early as 8 hr after drug treatment. Cells were seeded in 6-well plates in the presence of 5 μg/ml of erastin, 20 μg/ml of RSL5, or 0.5 μg/ml of RSL3. Cell viability was determined by Trypan Blue exclusion after 4, 8, 11, 12, and 13 hr of drug treatment. The graph is a representative outcome of twice experiments.

Figure 6. The Selective Lethality of RSL3 Is Not Confined to Mutant HRAS-Containing Cancer Cell Lines

(A) RSL3 was active in killing four KRAS mutation harboring cancer cells. A549, Calu-1, PaCa-2, and HCT116 cells were treated with RSL3 in 384-well plates for 24 hr. Percent growth inhibition was calculated with alamar blue. Error bars indicate one standard deviation of triplicate data.

(B) The activity of RSL3 was tested in 60 different human cancer cell lines. The left chart shows the result of 18 cell lines consisting of representative sensitive and resistant groups. Zero viability indicates a cytostatic effect of a compound, whereas negative viability indicates a cytotoxic effect. The right table shows results of the COMPARE analysis for paclitaxel and RSL3. The sensitivity profile of paclitaxel across 60 cancer cell lines has a strong correlation with those of other microtubule modulating agents. However, the top scored PCC value for RSL3 was 0.503, suggesting that RSL3 has a distinct sensitivity profile compared to other anticancer agents.

(C) Attenuating RAS signaling in Calu-1 cells by infecting with lentivirus containing shRNAs targeting *H*, *N*, or *KRAS* confers resistance to RSL3-induced lethality. Virus-infected cells were seeded in 384-well plates and treated with RSL3 for 24 hr. Percent growth inhibition was determined with alamar blue. Error bars indicate one standard deviation of triplicate data.

sufficient degree of promiscuity in their interaction with small-molecule ligands to enable multiple scaffolds to target these proteins.

One interesting shared property of RSLs is their iron-dependent mechanism of action. Many cancer cells are reported to have an enriched iron pool (Shterman et al., 1991); cancer patients have higher levels of iron than normal individuals (Stevens et al., 1988). Our BJ cell system captured this relationship between iron and cancer as BJ-TERT/LT/ST/RAS[V12] cells have more iron than their isogenic, nontumorigenic counterparts (Figure 7B). The greater iron content in BJ-TERT/LT/ST/RAS[V12] cells, together with the iron-dependent action of RSLs, lead us to the idea that the increased iron pool within cancer cells might be a target for inducing cancer-cell-specific lethality. Indeed, investigators have explored this possibility by testing iron chelators for anticancer properties (Kalinowski and Richardson, 2005). A number of iron chelators are reported to have good potency in inhibiting cancer cell growth.

Erastin and RSL5 exploit VDAC3 to induce synthetic lethality with oncogenic RAS. VDACs (VDAC1, VDAC2, and VDAC3) are mitochondrial pores that transport ions and small metabolites, including NADH, citrate, and succinate (Lemasters and Holmuhamedov, 2006). The use of VDACs as cancer-cell-selective drug targets has not been addressed, except in our previous report of erastin-induced, nonapoptotic, oxidative cell death. The presence of a compound, RSL5, that uses VDACs to induce selective lethality in oncogenic-RAS-containing cancer cells emphasizes the importance of VDACs as novel targets with a

---

(B) Time-dependent effect of RSL3 on BJ-TERT, BJ-TERT/LT/ST, and BJ-TERT/LT/ST/RAS[V12] cells. Cells were seeded in 6-well plates in the presence of the increasing concentration of RSL3. After 24, 48, and 72 hr, the number of viable cells was determined by using a Vi-Cell, and percent growth inhibition was calculated. Bar graph is a representative outcome of multiple independent experiments.

(C) Photograph of BJ-TERT and BJ-TERT/LT/ST/RAS[V12] cells treated with 5 μg/ml of erastin, 20 μg/ml of RSL5, 0.5 μg/ml of RSL3, or 1 μM of staurosporine for 24 hr.

(D) Staurosporine-treated but not erastin-treated, RSL5-treated, or RSL3-treated BJ-TERT/LT/ST/RAS[V12] cells contain the PARP-1 fragment produced by caspase-3/7 cleavage. Lysates of each treated samples were prepared. Ten micrograms of each lysate was analyzed by western blot with an antibody directed against human PARP-1.
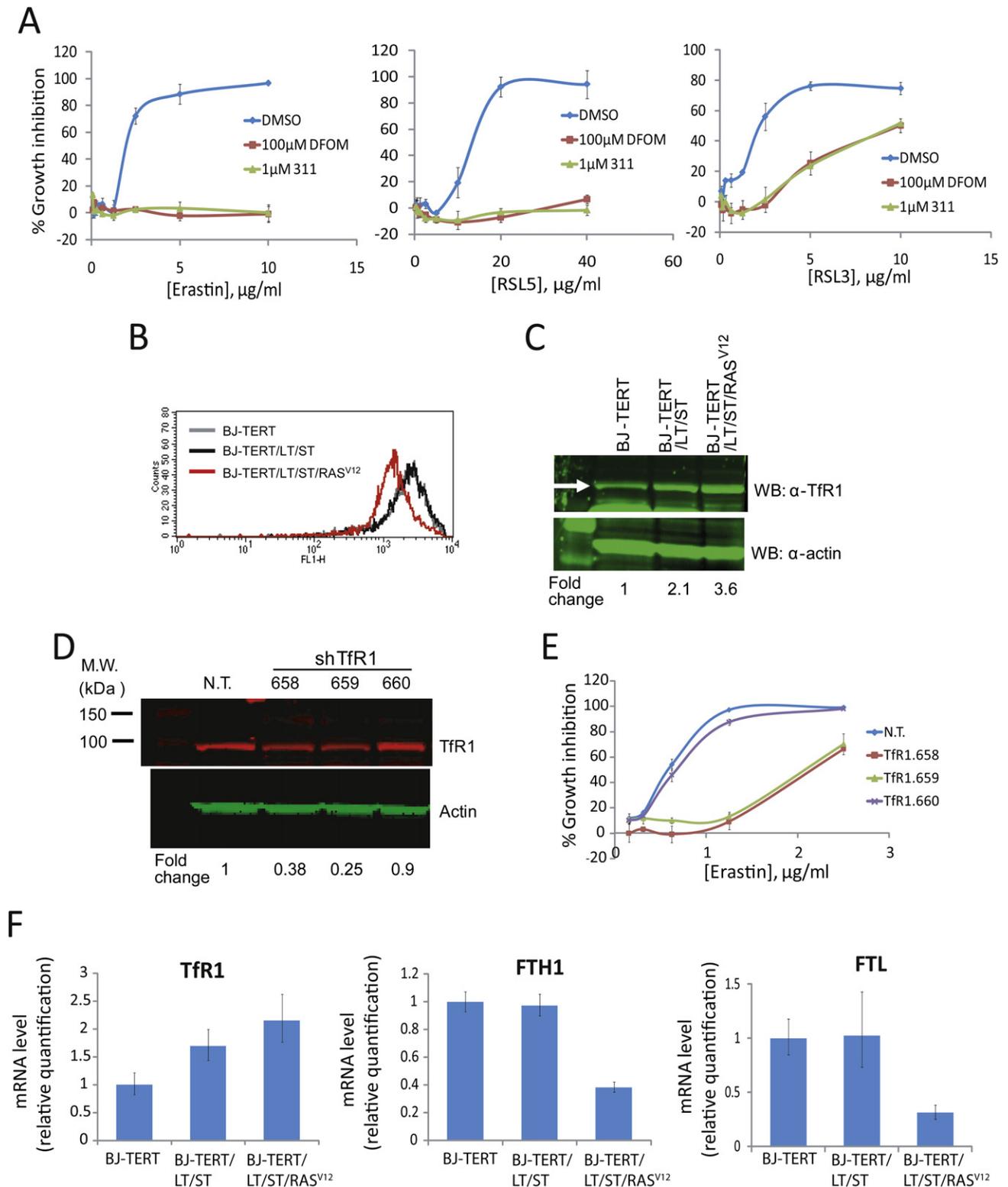
Figure 7. Oncogenic RAS Signaling Increases the Cellular Iron Content by Modulating Expression of *TfR1*, *FTH*, and *FTL*

(A) Iron chelators with different structures were able to suppress erastin-induced, RSL5-induced, and RSL3-induced cell death. BJ-TERT/LT/ST/RAS[V12] cells were treated with erastin (left), RSL5 (center), or RSL3 (right) in the presence or absence of iron chelators. Value represents the mean ± SD of triplicate data.

(B) BJ-TERT/LT/ST/RAS[V12] cells have a greater basal iron pool than their isogenic counterparts. BJ-TERT, BJ-TERT/LT/ST, BJ-TERT/LT/ST/RAS[V12] cells were stained with PGSK, and the fluorescence profile of stained cells was analyzed by flow cytometry.

For example, bleomycin, a key component of standard chemotherapeutic regimens for treating patient with germ-cell tumors (Kondagunta and Motzer, 2006), is known to oxidatively damage DNA through its complex with iron (Dorr, 1992). Another iron chelator, Triapine, entered phase II clinical trials in a combination therapy with cisplatin to treat ovarian cancer (Low and Schoenfeldt, 2005).

The increased iron concentration in BJ-TERT/LT/ST/RAS^{V12} cells compared to their isogenic counterparts raised the possibility that oncogenic-RAS signaling alters iron metabolism to augment the cellular labile iron pool (Figure 7B). Oncogene-induced increases in cellular iron have been reported for c-myc and E1A (Tsuji et al., 1995; Wu et al., 1999). Oncogenic signals from c-myc or E1A downregulate expression of the heavy subunit of ferritin (FTH1), which is a subunit of iron storage complex. Since ferritin functions as an iron buffer, downregulation of ferritin by oncogenic signals may result in an increased labile intracellular iron pool. Consequently, proliferation-driving enzymes, such as ribonucleotide reductase, are replenished with sufficient iron to function.

Oncogenic RAS has been proposed to enrich the cellular iron pool mainly by upregulation of *TfR1* expression. The existence of a mitogen-responsive element in the 5′ untranslated region (UTR) of *TfR1* mRNA has been reported, indicating that RAS-RAF-MEK-MAPK signaling may upregulate *TfR1* (Casey et al., 1988; Ouyang et al., 1993). Our data are consistent with this hypothesis; BJ-TERT/LT/ST/RAS^{V12} cells have increased mRNA and protein levels of *TfR1* compared to BJ-TERT and BJ-TERT/LT/ST cells (Figures 7C and 7F). In addition to this TfR1-mediated pathway, we found that oncogenic RAS downregulates *FTH1* and *FTL* to decrease the capacity of ferritin iron storage (Figure 7F). As c-myc and E1A were reported to downregulate *FTH1* expression, it would be interesting to test whether ferritin downregulation is a common means to enrich the cellular iron pool by oncogenes. Moreover, efforts to identify target proteins of RSL3 may ultimately reveal novel proteins in iron metabolism regulation; some such proteins are likely to be connected to RAS signaling.

These data demonstrate that synthetic lethal screening makes it possible to identify small molecules with enhanced lethality toward oncogene-harboring cancer cells, without targeting the oncogene itself. This feature of synthetic lethal screening becomes useful when we seek drug leads targeting loss of function cancer mutations, such as RAS, or tumor suppressors. Mechanism of action studies with these small molecules may lead to discovery of novel pharmacological targets for treating cancer and elucidation of critical connections between the targets and the cancer genes of interest; this should allow for a refined diagram of signaling networks in tumor cells.

SIGNIFICANCE

Synthetic lethal screening using small molecules involves testing compounds for selective lethality in tumor cells harboring a specific oncogenic mutation. While small molecules identified from target-based, in vitro screening directly inhibit function of a fixed target, small molecules identified from synthetic lethal screening do not perturb the function of the mutated gene; they "synthesize" lethality by targeting a protein component within the signaling network of the mutated gene. Therefore, small molecules identified from synthetic lethal screens are useful in identifying novel components of signaling networks of interest. We used oncogenic RAS (HRAS^{G12V}) as a specific mutation in synthetic lethal screening and identified two compounds, RSL5 and RSL3, whose activity depends on oncogenic RAS signaling. In order to define the mechanism of action for these compounds, we carried out counter screening with biologically active compounds to find suppressors of cell death induced by RSL5, RSL3, and erastin, a previously identified oncogenic-RAS-signal-dependent lethal compound. The efforts resulted in the identification of MEK, iron, reactive oxygen species, protein synthesis, and other kinases as selectivity-determining factors for each compound. Comparison of selectivity-determining factors among these compounds allowed us to reveal that RSL5, like erastin, acts through VDAC3 and provided some mechanistic insight into the action of RSL3. The counter screening also revealed that cellular iron is an important factor in inducing synthetic lethality with oncogenic RAS. Further analysis revealed that oncogenic RAS upregulates *TfR1* and downregulates *FTH1* and *FTL* to increase the labile iron pool. In conclusion, we identified two compounds from synthetic lethal screening involving oncogenic RAS, presented a means of using biologically active compounds to study the mechanisms of these compounds' action, and used these oncogenic-RAS-signal-dependent compounds to understand how oncogenic RAS enriches the cellular iron pool, which is an important factor for enabling oncogenic-RAS-selective lethality.

EXPERIMENTAL PROCEDURES

Please see the Supplemental Experimental Procedures for detailed descriptions of screening procedures and lentivirus production.

Cell Lines

BJ-fibroblast-derived cell lines were grown in a 4:1 mixture of DMEM to M199 supplemented with 15% heat-inactivated fetal bovine serum. The human fibrosarcoma cell line HT1080 was maintained in DMEM supplemented with

---

(C) BJ-TERT/LT/ST/RAS^{V12} cells have more TfR1 protein than that in their isogenic counterparts. Lysates of BJ-TERT, BJ-TERT/LT/ST, and BJ-TERT/LT/ST/RAS^{V12} cells were analyzed by western blot with an antibody directed against TfR1. We included an antibody directed against actin for assessing protein loading amount.

(D–E) Knocking down *TfR1* in BJ-TERT/LT/ST/RAS^{V12} cells partially inhibits cell death induced by erastin. Whole-cell lysates from BJ-TERT/LT/ST/RAS^{V12} cells infected with either nontargeting shRNA (N.T.) or three different *TfR1*-targeting shRNAs (658, 659, 660) were prepared, and the level of TfR1 in each cell line was determined by western blot with an antibody against TfR1 (D). The same set of cell lines was treated with indicated concentration of erastin and percent growth inhibition was determined with alamar blue (E). Error bars indicate one standard deviation of triplicate data.

(F) Oncogenic RAS upregulates *TfR1* but downregulates *FTH1* and *FTL*. Cellular RNAs were prepared from each cell line, and real-time PCR was performed with each gene-specific primer set. The expression levels of *TfR1*, *FTH1*, and *FTL* were first normalized to the level of endogenous control (*RPLPO*). The relative expression level of each gene among the three cell lines was expressed as a ratio of transcripts in a cell line to those in BJ-TERT. Value represents the mean ± SD of three measurements of each sample.

nonessential amino acids and 10% calf serum. The human lung carcinoma cell line Calu-1 and colon carcinoma cell line HCT116 were grown in McCoy's 5A medium supplemented with 10% calf serum. A human lung carcinoma cell line A549 was grown in DMEM supplemented with 10% calf serum. The human pancreatic carcinoma cell line MIA PaCa-2 was maintained in DMEM supplemented with 10% calf serum and 2.5% horse serum. Penicillin and streptomycin were used as antibiotics in all media.

Compound Libraries

Chemical libraries were composed of a combination of synthetic and natural product-like compounds. In total, 47,725 small molecules were obtained from different providers; 2,056 from TimTec, 8,669 from IBS, 17,520 from Chembridge, 12,240 from Asinex, 5,240 from Life chemicals, and 2,000 from MicroSource Discovery. All compounds were prepared as 4 mg/ml solutions in DMSO in 384-well polypropylene plates (Greiner, cat. #781280) and stored at $-80°C$. We refer to these plates as mother plates.

Viability Assay

Alamar Blue Assay

After 24 or 48 hr of compound treatment, 10 μl of 50% alamar blue solution in growth medium was transferred to the assay plates, which resulted in 10% final concentration alamar blue. Plates were incubated further for 16 hr to allow reduction of alamar blue, which results in the generation of red fluorescence. The fluorescence intensity was determined by using a Victor 3 plate reader (Perkin Elmer) with a 535 nm excitation filter and a 590 nm emission filter.

Trypan Blue Assay

200,000 cells were seeded in 6-well plates and treated with indicated amount of 2-fold dilution series concentration of compound in 2 ml BJ growth medium. After 24 hr, cells were released with trypsin/EDTA, harvested in 1.1 ml growth medium, and transferred to Vi-Cell (Beckman Coulter) disposable cup. Trypan blue staining, taking 100 images of sample and analysis of the images were carried out automatically by the Vi-Cell.

Counter Screening with Iron Chelators

BJ-TERT/LT/ST/RAS[V12] cells were seeded in 384-well assay plates at a concentration of 4,000 cells per well in 32 μl volume. Cells were treated with iron chelators by transferring 4 μl of 1 mM deferoxamine mesylate (Calbiochem, cat. #252750), or 125 μM compound 311 (Chembridge, cat. #5135701) in growth media to the assay plate. Then, we transferred 4 μl from the "10× lethal plate" (described in Counter Screening with Biologically Active Compounds in the Supplemental Experimental Procedures) to the assay plate in order to induce cell death. Assay plates were incubated for 24 hr, and alamar blue was added to the plates at a final concentration of 10%.

Monitoring Cellular Iron Level Using Flow Cytometry

Cells were seeded in 6-well plates (200,000 cells per well) in BJ medium. The next day, the cell monolayer was washed with PBS twice and stained with 5 μM of Phen Green SK, diacetate (Molecular Probe, cat. #P14313) in PBS by incubating the plate for 15 min in culture incubator. Cells were released with trypsin/EDTA, harvested in 2 ml PBS, and centrifuged at 1,000 rpm for 5 min. The cell pellet was resuspended in 1 ml of PBS, the cell suspension was transferred to disposable FACS tubes, and fluorescence profile of the sample was monitored by using a FACSCalibur system (BD Biosciences).

Western Blot

Monitoring Cleavage of PARP1 and Caspase-3 upon Compound Treatment

2×10^6 BJ-TERT/LT/ST/RAS[V12] cells were seeded in 10 cm dishes and treated with 1 μM staurosporine, 10 μg/ml erastin, 20 μg/ml RSL5, and 1 μg/ml RSL3 for 16 hr. Both dying cells and live cells in each 10 cm dish were harvested and collected in the same 15 ml tubes by centrifuging cell suspension at 1,000 rpm for 5 min. Cell pellets were washed three times with PBS, and cells were lysed in 200 μl of denaturing lysis buffer (50 mM HEPES KOH [pH 7.4], 40 mM NaCl, 2 mM EDTA, 1.5 mM Na_3VO_4, 50 mM NaF, 10 mM sodium pyrophosphate, 10 mM sodium β-glycerophosphate, 0.5% Triton X-100, and protease inhibitor tablet [Roche, cat. #11836170001]). Protein content was quantified by using a Bio-Rad protein assay reagent (Bio-Rad, cat. #500-00006). Equal amounts of protein were resolved on SDS-polyacrylamide

gels. The electrophoresed proteins were transblotted onto a PVDF membrane, blocked with 5% milk, and incubated with rabbit primary antibodies specific to: PARP (Santa Cruz, cat. #sc-7150), cleaved caspase-3 (Cell Signaling Technology, cat. #9661) overnight at 4°C. The membrane was then incubated in IRDye 800 goat anti-rabbit antibody (Li-Cor Bioscience cat. #926-32211) at 1:3,000 dilutions for 45 min at room temperature. After washing off the unbound antibodies, membranes were scanned with the Odyssey Imaging System (Li-Cor Bioscience).

Basal Expression Level of TfR1

BJ-TERT, BJ-TERT/LT/ST, and BJ-TERT/LT/ST/RAS[V12] cells were seeded prior to the experiment in 10 cm dishes and allowed to grow to 80% confluence. The cell monolayer was washed three times with PBS, and cells were lysed in 200 μl of denaturing lysis buffer. The cell lysates were subjected to western blot analysis as described above. An antibody directed against human transferrin receptor 1 (Santa Cruz, cat. #sc-7087) was used.

Monitoring Drug Sensitivity in shRNA-Expressing Cells

HT1080 or Calu-1 cells were infected with lentiviruses that contain shRNA expression plasmids as described in the Supplemental Experimental Procedures. On the day of experiment, assay plates were prepared by seeding 1,500 shRNA-infected cells per well in 36 μl of growth media to black, clear-bottom 384-well plates. Cells in the assay plates were treated with each lethal compound in a 2-fold dilution series by transferring 4 μl solution from a 10× lethal plate of erastin, RSL5, RSL3, or staurosporine. Assay plates were returned to the culture incubator and maintained for 24 hr before adding alamar blue. Percent growth inhibition (% GI) was calculated with fluorescence intensity values.

Real-Time RT-PCR

Total RNA was extracted with RNeasy kit (QIAGEN, cat. #74104) as described in the manufacturer's handbook. One microgram of RNA sample was subject to reverse transcription reaction by using TaqMan Reverse Transcription Reagents (Applied Biosystems, cat. #N8080234) according to the manufacturer's instruction. Then, Q-PCR was carried out by using Power SYBR Green PCR Master Mix (Applied Biosystems, cat. #4367659) and 7300 Real-Time PCR System (Applied Biosystems). The sequence of primers for Q-PCR is shown in the Supplemental Data.

SUPPLEMENTAL DATA

Supplemental Data include Supplemental Experimental Procedures, four figures, one table, and sequence of primes used and can be found with this article online at http://www.chembiol.com/cgi/content/full/15/3/234/DC1/.

REFERENCES

Banerjee, D., Schnieders, B., Fu, J.Z., Adhikari, D., Zhao, S.C., and Bertino, J.R. (1998). Role of E2F-1 in chemosensitivity. Cancer Res. 58, 4292–4296.

Bernards, A. (2005). Ras superfamily and interacting proteins database. Methods Enzymol. 407, 1–9.

Bryant, H.E., Schultz, N., Thomas, H.D., Parker, K.M., Flower, D., Lopez, E., Kyle, S., Meuth, M., Curtin, N.J., and Helleday, T. (2005). Specific killing of BRCA2-deficient tumours with inhibitors of poly(ADP-ribose) polymerase. Nature 434, 913–917.

Casey, J.L., Di Jeso, B., Rao, K., Rouault, T.A., Klausner, R.D., and Harford, J.B. (1988). The promoter region of the human transferrin receptor gene. Ann. N Y Acad. Sci. 526, 54–64.

Cheng, Y., Zak, O., Aisen, P., Harrison, S.C., and Walz, T. (2004). Structure of the human transferrin receptor-transferrin complex. Cell 116, 565–576.

Dolma, S., Lessnick, S.L., Hahn, W.C., and Stockwell, B.R. (2003). Identification of genotype-selective antitumor agents using synthetic lethal chemical screening in engineered human tumor cells. Cancer Cell 3, 285–296.

Dorr, R.T. (1992). Bleomycin pharmacology: mechanism of action and resistance, and clinical pharmacokinetics. Semin. Oncol. 19, 3–8.

Green, D.A., Antholine, W.E., Wong, S.J., Richardson, D.R., and Chitambar, C.R. (2001). Inhibition of malignant cell growth by 311, a novel iron chelator of the pyridoxal isonicotinoyl hydrazone class: effect on the R2 subunit of ribonucleotide reductase. Clin. Cancer Res. 7, 3574–3579.

Hahn, W.C., Counter, C.M., Lundberg, A.S., Beijersbergen, R.L., Brooks, M.W., and Weinberg, R.A. (1999). Creation of human tumour cells with defined genetic elements. Nature 400, 464–468.

Hahn, W.C., Dessain, S.K., Brooks, M.W., King, J.E., Elenbaas, B., Sabatini, D.M., DeCaprio, J.A., and Weinberg, R.A. (2002). Enumeration of the simian virus 40 early region elements necessary for human cell transformation. Mol. Cell. Biol. 22, 2111–2123.

Harrison, P.M., and Arosio, P. (1996). The ferritins: molecular properties, iron storage function and cellular regulation. Biochim. Biophys. Acta 1275, 161–203.

Hartwell, L.H., Szankasi, P., Roberts, C.J., Murray, A.W., and Friend, S.H. (1997). Integrating genetic approaches into the discovery of anticancer drugs. Science 278, 1064–1068.

Kalinowski, D.S., and Richardson, D.R. (2005). The evolution of iron chelators for the treatment of iron overload disease and cancer. Pharmacol. Rev. 57, 547–583.

Kondagunta, G.V., and Motzer, R.J. (2006). Chemotherapy for advanced germ cell tumors. J. Clin. Oncol. 24, 5493–5502.

Lemasters, J.J., and Holmuhamedov, E. (2006). Voltage-dependent anion channel (VDAC) as mitochondrial governator–thinking outside the box. Biochim. Biophys. Acta 1762, 181–190.

Low, J.A., and Schoenfeldt, M. (2005). Clinical trials referral resource. Current clinical trials investigating 3-AP. Oncology 19, 354, 357–358.

Moffat, J., Grueneberg, D.A., Yang, X., Kim, S.Y., Kloepfer, A.M., Hinkle, G., Piqani, B., Eisenhaure, T.M., Luo, B., Grenier, J.K., et al. (2006). A lentiviral RNAi library for human and mouse genes applied to an arrayed viral high-content screen. Cell 124, 1283–1298.

Neshat, M.S., Mellinghoff, I.K., Tran, C., Stiles, B., Thomas, G., Petersen, R., Frost, P., Gibbons, J.J., Wu, H., and Sawyers, C.L. (2001). Enhanced sensitivity of PTEN-deficient tumors to inhibition of FRAP/mTOR. Proc. Natl. Acad. Sci. USA 98, 10314–10319.

Nociari, M.M., Shalev, A., Benias, P., and Russo, C. (1998). A novel one-step, highly sensitive fluorometric assay to evaluate cell-mediated cytotoxicity. J. Immunol. Methods 213, 157–167.

Ouyang, Q., Bommakanti, M., and Miskimins, W.K. (1993). A mitogen-responsive promoter region that is synergistically activated through multiple signalling pathways. Mol. Cell. Biol. 13, 1796–1804.

Paull, K.D., Shoemaker, R.H., Hodes, L., Monks, A., Scudiero, D.A., Rubinstein, L., Plowman, J., and Boyd, M.R. (1989). Display and analysis of patterns of differential activity of drugs against human tumor cell lines: development of mean graph and COMPARE algorithm. J. Natl. Cancer Inst. 81, 1088–1092.

Petrat, F., de Groot, H., and Rauen, U. (2000). Determination of the chelatable iron pool of single intact cells by laser scanning microscopy. Arch. Biochem. Biophys. 376, 74–81.

Rodenhuis, S. (1992). ras and human tumors. Semin. Cancer Biol. 3, 241–247.

Shterman, N., Kupfer, B., and Moroz, C. (1991). Comparison of transferrin receptors, iron content and isoferritin profile in normal and malignant human breast cell lines. Pathobiology 59, 19–25.

Smith, M.R., DeGudicibus, S.J., and Stacey, D.W. (1986). Requirement for c-ras proteins during viral oncogene transformation. Nature 320, 540–543.

Stevens, R.G., Jones, D.Y., Micozzi, M.S., and Taylor, P.R. (1988). Body iron stores and the risk of cancer. N. Engl. J. Med. 319, 1047–1052.

Stockwell, B.R. (2000). Chemical genetics: ligand-based discovery of gene function. Nat. Rev. Genet. 1, 116–125.

Tong, A.H., Evangelista, M., Parsons, A.B., Xu, H., Bader, G.D., Page, N., Robinson, M., Raghibizadeh, S., Hogue, C.W., Bussey, H., et al. (2001). Systematic genetic analysis with ordered arrays of yeast deletion mutants. Science 294, 2364–2368.

Tsuji, Y., Akebi, N., Lam, T.K., Nakabeppu, Y., Torti, S.V., and Torti, F.M. (1995). FER-1, an enhancer of the ferritin H gene and a target of E1A-mediated transcriptional repression. Mol. Cell. Biol. 15, 5152–5164.

Varma, H., Voisine, C., DeMarco, C.T., Cattaneo, E., Lo, D.C., Hart, A.C., and Stockwell, B.R. (2007). Selective inhibitors of death in mutant huntingtin cells. Nat. Chem. Biol. 3, 99–100.

Wilhelm, S., Carter, C., Lynch, M., Lowinger, T., Dumas, J., Smith, R.A., Schwartz, B., Simantov, R., and Kelley, S. (2006). Discovery and development of sorafenib: a multikinase inhibitor for treating cancer. Nat. Rev. Drug Discov. 5, 835–844.

Wu, K.J., Polack, A., and Dalla-Favera, R. (1999). Coordinated regulation of iron-controlling genes, H-ferritin and IRP2, by c-MYC. Science 283, 676–679.

Yagoda, N., von Rechenberg, M., Zaganjor, E., Bauer, A.J., Yang, W.S., Fridman, D.J., Wolpaw, A.J., Smukste, I., Peltier, J.M., Boniface, J.J., et al. (2007). RAS-RAF-MEK-dependent oxidative cell death involving voltage-dependent anion channels. Nature 447, 864–868.